18th ESV Paper

THE DEVELOPMENT OF AN INJURY CRITERIA FOR AXIAL LOADING TO THE THOR-LX BASED ON PMHS TESTING

David Hynd
Claire Willis
Adrian Roberts
Richard Lowne
TRL Limited
UK

Richard Hopcroft
Paul Manning
WA Wallace
The University of Nottingham
UK

Paper Number 078

ABSTRACT

Many accident studies have shown that lower leg injuries are common in frontal impact car accidents. Of these, injuries to the ankle are the most serious and the most likely to lead to long-term morbidity.

Fourteen PMHS specimens were impacted using a new double-impact sled rig that loads the leg in a realistic, car-equivalent manner. The sled separately reproduces the vehicle deceleration and footwell intrusion typically seen in frontal impacts.

The impacts were at a range of foot loading severities, with a constant-force knee restraint and Achilles tendon tension applied such as to reproduce the emergency braking forces found in simulator studies. Only one impact was applied to each specimen, which was then examined for injury by x-ray and necropsy.

The injuries generated were considered to be representative of those seen in car accidents. Tests at each severity were then replicated with a THOR-Lx lower leg and an injury risk curve for the THOR-Lx is presented.

INTRODUCTION

A number of accident analyses have shown that very disabling lower leg injuries frequently result from frontal impacts and that they form a significant part of the total burden of road traffic accidents [Pilkey et al., 1994; Otte, 1996; Martin et al., 1997]. [Pattimore et al., 1991] reported that of the survivors in frontal accidents in the CCIS database, the lower limbs were the most frequently injured body area, with the majority of injuries to the foot and ankle. For AIS 2 and 3 injuries, the lower limbs were second only to the head and face. Airbags have reduced the incidence of severe head and thorax injuries, but there has not been a reduction in lower leg injuries [Burgess et al., 1995; Crandall et al., 1996]. Indeed, some studies have indicated an increased incidence of lower leg injury in the presence of an airbag deployment [Owen and Hynd, 2001].

Axial loading has been identified as the cause of the majority of impairing injuries to the ankle and hind-foot [Morris et al., 1997; Sherwood et al., 1999]. Thus the purpose of this work was to investigate the risk of injury to the foot and ankle under axial loading in a manner representative of that found in a frontal car crash. Previous work by our group was directed towards developing an understanding of the mechanism of injury of the types of foot and ankle injury regarded as being the highest priority for prevention. Priority was assigned from accident analysis data, not on the basis of injury frequency but of long-term disability, ascertained by impairment scoring. The priorities were pilon, calcaneal and talar neck fractures, as all are difficult to treat clinically and have a poor outcome [Taylor et al., 1997]. Calcaneal and pilon fractures are relatively common and are particularly disabling as they usually involve disruption of the articular surface of a weight-bearing joint. Joint cartilage is not vascularised and biological repair only occurs by fibrous replacement, so healing is often poor, resulting in long-term complications such as infection, malunion and osteoarthritis [Funk et al., 2001]. Talar neck fractures have similarly poor outcomes due to the development of avascular necrosis of the dome of the talus following fracture at the neck where the only blood supply to the dome is located.

PMHS (Post Mortem Human Subject) tests by our group have included the application of concentrated loads to different parts of the foot of fully restrained below-knee fresh-frozen specimens via a linear impactor [McMaster et al., 2000]. Calcaneal, talar neck and pilon fractures were generated in high-rate loading conditions. In addition to the impactor load, the Achilles tendon was tensioned to various loads as this was expected to affect the threshold for injury. It was found that the Achilles tension was significantly higher in the pilon and talar neck fracture group than in the calcaneus fracture group, although the BMD (Bone Mineral Density) of the calcaneus group was lower. Other authors have indicated that increased Achilles tension reduces the overall risk of an injury occurring in PMHS tests, but that it increases the likelihood of pilon fracture

[Funk et al., 2001]. It is expected that braking or bracing are likely to be a factor in the majority of frontal impacts, thus Achilles tension is likely to be present.

Appropriate injury types were generated and an understanding of the role of Achilles tension in injury was developed. However, when the tests were repeated with a Hybrid III leg, unrealistically high axial forces were measured [McMaster et al., 2000]. Forces of this magnitude would not be seen in a frontal impact vehicle crash because the foot and leg would have moved away from the loading surface before such high forces could be generated. In order to calibrate the dummy leg and derive an injury risk curve, it was apparent that a more realistic loading environment would have to be used. To address this need, a new sled-based test rig has been designed that allows the foot and leg to be correctly loaded and to react in a manner representative of the in-car situation. This paper presents the design of the sled rig and the test protocol used, along with the PMHS test programme and an analysis of the injuries induced. The tests were then repeated with a THOR-Lx (GESAC, Inc) to establish an injury risk curve for foot and ankle injuries to be used with this test device.

Seven fresh-frozen PMHS specimens were subjected to a total of ten tests in a pilot programme to refine and validate the test protocol and 15 fresh-frozen specimens were subjected to a total of 16 tests in the main test programme. The specimen that was impacted twice was subjected to a moderate load in one test that did not allow proper intrusion of the foot-plate due to equipment failure. It was then impacted, correctly, a second time, but was excluded from the injury risk analysis and is not reported further because the effect of the first impact on the likelihood of injury in the second impact was not known

METHOD

Test Configuration

Background

In a frontal impact, the foot and leg are subjected to a global deceleration phase due to the deceleration of the vehicle. They are then subjected to a much higher force due to intrusion of the footwell. During the first phase of deceleration, the foot is restrained by the footwell or pedal and the pelvis moves forward until restrained by the seat belt. This causes inertial loads to be applied to the leg. The footwell or pedal intrusion then loads the leg much more severely. It was considered that the initial inertial loading could be important in the mechanism of injuries seen in road traffic accidents as it would compress the bones of the foot and ankle together prior to the main loading from the footwell intrusion. Any bracing or braking effort would be expected to stiffen further the foot and ankle joints [McMaster et al., 2000].

Solid body modelling (Madymo) was used to investigate a number of possible methods of replicating this in-car loading regime. It was not possible to reproduce the target pulse satisfactorily with an impact to a stationary leg. Instead, it was found to be necessary to reproduce the global deceleration pulse of the vehicle as well as the impact pulse to the leg from the footwell. This gave the inertial as well as impact loading to the leg, and allowed the leg to react to the impact in a vehicle realistic manner.

The sled pulse was based on a number of frontal offset car crash tests with mid-size saloon cars (Figure 1). This shows a fairly constant 20 g pulse for 25 ms, followed by a much higher intrusion pulse, such as to give a peak force of up to 10 kN over a period of 10 ms. This agrees well with the form of the pulses reported in Krüger [1994] and Sakurai [1996].

In order to derive an injury risk curve, tests at injury and non-injury levels are required. It was decided to vary the severity of the tests by altering the severity of the footwell intrusion part of the pulse, while keeping the vehicle deceleration part of the pulse constant. This represents different car performances in the same severity of collision. The pulse given in Figure 1 represents a high severity impact.

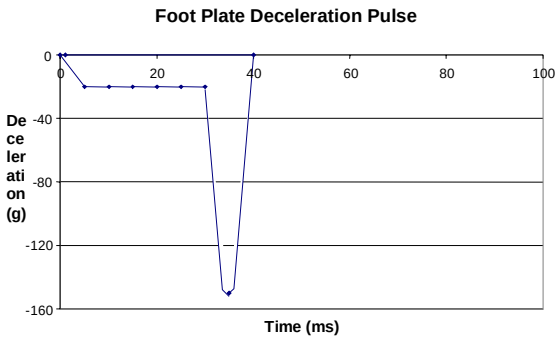

Figure 1. Idealised frontal impact footwell pulse.

Sled Rig

The new sled rig was designed to enable testing of PMHS limbs at a range of impact severities. The sled recreates the deceleration profile of an occupant's pelvis, with intrusion and limb displacement relative to the pelvis. The design specification was modelled on the footwell and

pelvis recordings from a full-scale crash test using a standard mid-range car in frontal impact.

The rig consists of an elastic rope (bungee) powered sled (see Figure 2), firing down a test track, impacting into an aluminium honeycomb energy absorber (A). A simulated toe-pan or pedal unit (the foot-plate - B), mounted on the sled, is caused to intrude by impacting a second section of aluminium honeycomb (C). Figure 3 shows the THOR-Lx mounted on the sled in the same position as the PMHS specimens. By manipulating the position and properties of the aluminium honeycomb, the deceleration, amount of intrusion, and delay between impacts can be predetermined and reproduced. The design allows great versatility in tuning to the desired impact pulse. Impact speeds range from 7 $m.s^{-1}$ to 15 $m.s^{-1}$, generating sled decelerations ranging from 20 g to 50 g. Toe-pan accelerations of up to 200 g can be generated with intrusion capabilities of 0 to 200 mm. Repeat tests with a Hybrid III leg showed a very high level of test repeatability (see Figure 4), as did two low severity pilot tests with the same PMHS specimen (Figure 5).

Foot-plate Loading Interface

Funk [2001] reported that a number of studies indicated that localised impacts to the mid-foot were more likely to generate pilon fractures than localised loading to the calcaneus. However, they stated that compressive loading to the calcaneus was probably ubiquitous in severe frontal crashes. For this reason, it was suggested that a blunt impact to the entire plantar surface of the foot would provide the most realistic loading scenario. This was contrary to the authors' experience with crashed cars, which indicated that local deformations of the footwell were common and could be severe, either in magnitude of deformation (greater than 50 mm) or shape (sharp edges that could apply very localised loading to the foot). However, a flat foot-plate would be more straightforward experimentally and would simplify interpretation of the loading applied to the foot.

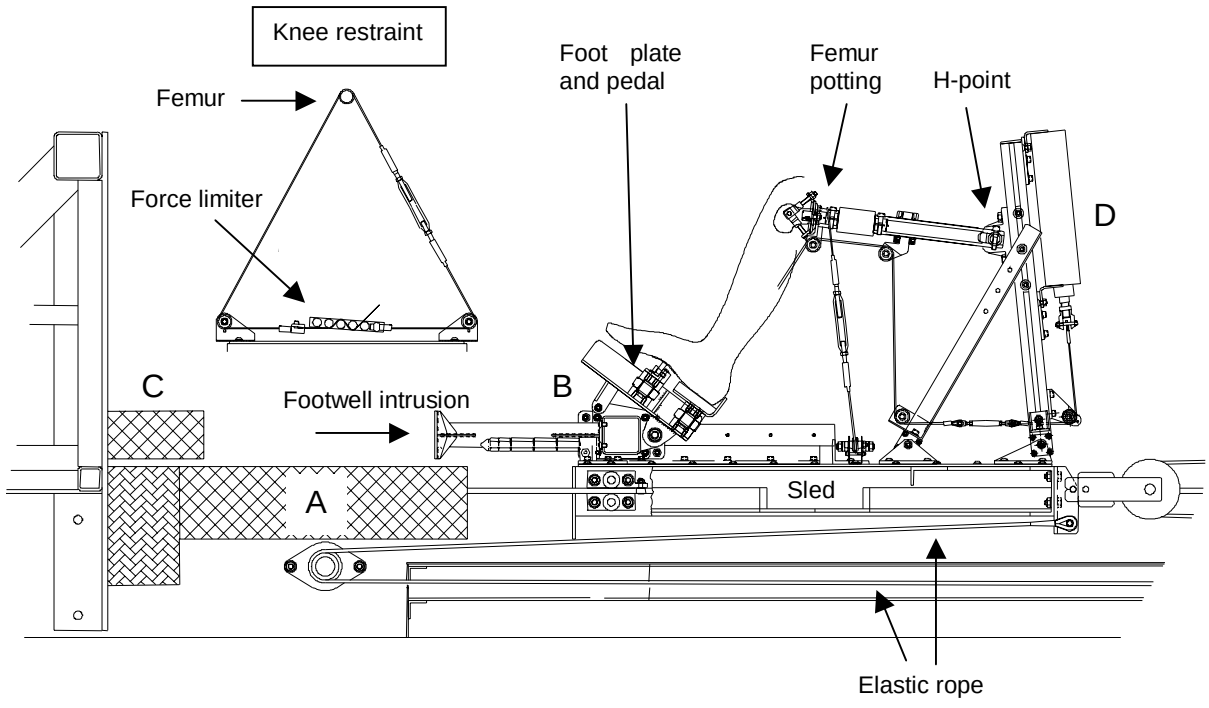

Figure 2. Schematic of sled showing the hip support, femur potting mechanism, Achilles tendon tensioning system, knee restraint and foot-plate with pedal. The inset shows a frontal view of the knee restraint system with a plan view of the friction device.

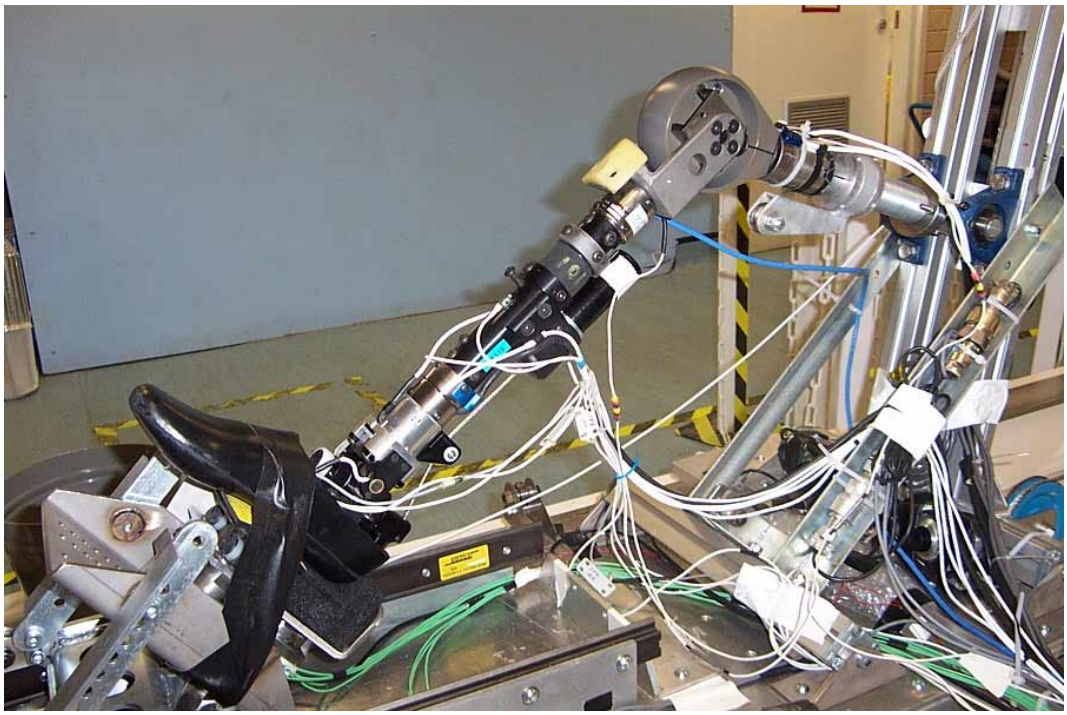

Figure 3. The THOR-Lx mounted on the sled in the same position as the PMHS specimens.

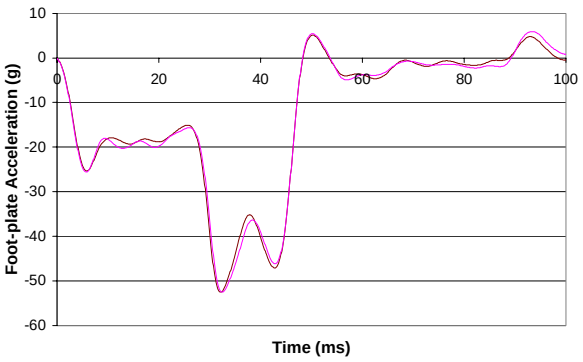

Figure 4. Two repeat tests with a Hybrid III leg.

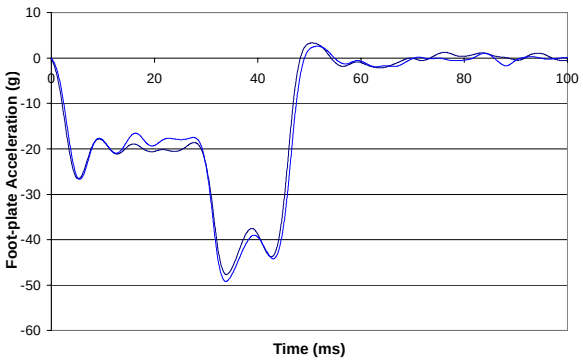

Figure 5. Two repeat tests with a single PMHS specimen.

Pilot tests were therefore conducted with a flat loading surface (no pedal representation) and with the heel and fore-foot in contact with the plate at impact. These tests produced injuries to the calcaneus that were of a type not seen clinically as a result of road traffic accidents. In each of the impacts in which this injury type occurred, examination of the high-speed cinematography demonstrated that the arch of the foot collapsed as the load was applied. It should be noted that the PMHS was not fitted with a shoe, which could help to maintain the arch of the foot, although a Velbex rubber sheet, representative of the stiffness of the sole of a shoe, was placed between the sole of the foot and the foot-plate. The impacts generated sufficiently high tension through the plantar fascia and long plantar ligaments to fracture their attachment to the antero-inferior cortex of the calcaneus. The deficiency thus created permitted extension of the fracture, propagating through the region of the sinus tarsi, effectively flexing the body of the calcaneus around the inferior talus. This represented a failure of the static stabilisers of the arch of the foot, namely the plantar ligaments and bony architecture. (In the living human the arch anatomy would be further supported dynamically, primarily by the action of tibialis anterior and tibialis posterior muscles and as a secondary action of the long flexors of the toes via their tendons. Without recreating these dynamic forces, the ability of the arch mechanism to transmit the load from the forefoot to the hind foot and ankle is severely restricted.) Thus, these impacts did not recreate accurately the function of the foot in a dynamic

setting and the injuries induced were not representative of those seen in road traffic accidents. Further pilot tests with a pedal representation under the ball of the foot yielded the same injury mechanism.

As a result of the pilot tests, a more direct axial load application was opted for. A replica brake pedal, based on the form and dimensions of a Saab 9000 automatic brake pedal, replaced the flat load plate. The position of the pedal, when the specimen was mounted, lay at the junction of mid and hind foot in the arch of the foot, with the lower edge of the pedal in line with the anterior tibial margin. This represented the position the foot may take while braking at the point immediately prior to intrusion of the foot well. Previous PMHS tests from this research group have shown this to be the impact position most likely to induce pilon and talar neck fractures, in addition to calcaneus fractures [McMaster et al., 2000]. Another study [Kitagawa et al., 1998] has shown that impacts in line with or just anterior to the anterior tibial margin, although the forces were not as concentrated as in the McMaster [2000] paper, are likely to cause these injuries. In addition, high-speed film of the footwell area in frontal impact car tests was reviewed. This showed the dummy's feet sliding forward during the initial vehicle deceleration phase until stopped by toe contact with the top of the footwell. This meant that the pedals were level with the mid-foot at the time of footwell intrusion and the position of the foot on the pedal used in these tests can be considered to be realistic.

Achilles Tendon Load

Previous PMHS work [Manning et al., 1997b; McMaster et al., 2000] had implemented Achilles tension, but it had proved to be difficult to connect to the tendon sufficiently well for the high forces involved to be sustained. With the test set-up for the current programme, the time elapsed between tensioning the tendon and impacting the foot was much greater than in the previous programmes and a more robust clamping technique was therefore required.

A new technique was developed whereby the tendon was double-clamped. The tendon was looped through an eyelet at the end of the tensioning cable and the two parts of the tendon were clamped together. A second clamp was then attached to the free end of the tendon just behind the first clamp. The whole assembly was then locally frozen using a freezer aerosol. This method proved to be very reliable and it was possible to maintain Achilles tension of up to 1.5 kN for over ten minutes with almost no loss of tension.

The Achilles tension was developed by a pressurised pneumatic cylinder mounted on the rear of the sled (D in Figure 1). Tension was applied in an anatomical direction, with the cable running inferior to the gastrocnemius. A small uniaxial load cell was mounted between the cable and the tendon clamp to measure the Achilles force both when setting-up the specimen and during the test.

Knee Brace

In addition to the simulation of Achilles tension, a knee brace was used to simulate the knee extension forces in pre-impact emergency braking (inset to Figure 2). The mechanism worked by pulling a strip of metal through a series of rollers to apply a constant force to resist hip flexion and thereby resist rearward motion of the foot. The knee restraint represented (in combination with the Achilles tension) the active muscular force in emergency braking, allowing a controlled movement of the specimen during impact. This was not equivalent to the restraint that would be caused by pocketing of the knee in the dashboard.

Anterior Draw Cable

Several of the specimens in the pilot series were found to have physiological atrophy or attenuation of the anterior cruciate ligament together with varying degrees of degenerative wear of the knee joint. These conditions resulted in a degree of instability in the joint. As a result of this instability, several of the pilot tests exhibited a posterior subluxation of the femur at the knee joint whilst setting the Achilles and knee restraint loads. In two pilot specimens there was complete disruption and posterior dislocation of the femoral condyles on the tibia at impact.

To counteract the instability, a static anterior draw stabilising cable was devised to supplement the action of the anterior cruciate ligament. A cable was looped around the exposed upper end of the tibia and attached to the femur mounting block. The knee retained a full range of physiological movement in both flexion-extension and rotation, without restriction.

Test Procedure

Specimen Selection

This PMHS study had full ethical approval[1]. The PMHS specimens were recovered after consent had

[1] This research was approved by the Ethical Committees of the Queen's Medical Centre, University of Nottingham, UK, The North Nottinghamshire Health Ethics committee and the National Ethical Committee of the British Medical Association.

been obtained and were treated and stored according to the SAE adopted protocol for the preservation of human surrogates for biomechanical testing [Crandall, 1994]. Screening prior to recovery excluded donations from individuals who had a history of previous trauma, long standing disease or period of prolonged pre-morbid bed rest. Each specimen was inspected for suitability and storage damage prior to its acceptance into the program. Radiological imaging and bone mineral density, using a Lunar-Expert DXA scanner, were assessed prior to testing.

Mounting Procedure

The PMHS specimens were recovered as an above knee amputation with a short (75 mm) femur section. In order to attach the specimen to the sled, a new attachment device had to be developed. Because of the high forces involved, the device consists of two attachments to the leg (see Figure 6). The first is a knurled spigot that is bonded into the medullary cavity of the femur (A on Figure 6)) in line with the longitudinal axis of the femur (B. The second attachment is a bar through the femoral condyles parallel to the axis of the tibio-femoral joint (C). The two attachments are joined with an angled framework (D), which is then attached to the sled via an articulated dummy femur (E). This attachment method has proved to be very robust, with only slight loosening of the femur bar in one of the pilot specimens.

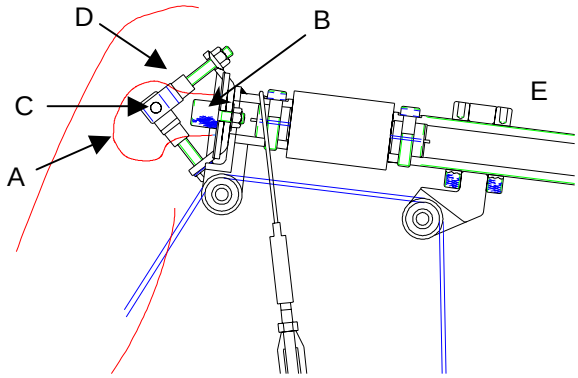

Figure 6. Detail of knee mounting bracket.

A crucial aspect of recreating a realistic impact in this study is the position of the specimen. The angle between the tibial axis and the axis of direction of travel is critical in determining the relative increase in inertial loading between the first and second phases of the impact in each test. A survey of seated drivers in cars was undertaken in order to determine the range of joint positions and angles. Each driver was requested to seat him or herself comfortably according to their usual driving style (position one). From this initial position, they were then requested to brake heavily, depressing the brake through its full excursion (position two). Then, each driver was positioned as far forward in the seat as possible until restricted by knee impingement with the dashboard (position three). Hip height, knee angle, ankle angle and the angle between the sole of the foot and the floor of the car were recorded for each driver in each of the three positions. The measurements for each driver were repeated in a range of mid-sized saloon cars. This produced forty-three different combinations of drivers and cars.

The position of the specimens was based on the mean positions of the subjects when braking heavily. The specimen was mounted to give initial ankle and knee angles of 90° and 124° respectively and a hip height above the top of the sled of 240 mm. The hip support system was adjustable to allow this initial position irrespective of the size of the specimen. The angle of the sole of the foot relative to the horizontal was 53° for all tests. This represented the position of the lower limb under braking, thus correctly orientating the tibia relative to the direction of intrusion.

Instrumentation

The sled was instrumented with two uni-axial accelerometers, mounted on the sled and foot-plate, as well as a string potentiometer to measure foot-plate displacement. Data from the accelerometers was used to tune the two deceleration pulses and to ensure that the pulses were maintained and repeatable throughout testing. Sled velocity was measured using a track-side infra-red timing device. Three tri-axial load cells were mounted under the foot, two under the pedal and one under the heel, to indicate the force exerted by the specimen and to ensure that the specimen was balanced following tensioning. Lateral and overhead high-speed cine cameras (400 frames/sec) were run for two seconds either side of impact.

A tri-axial accelerometer array was screwed to the second metatarsal of the foot in a position of best fit, within the proximal third of the bone. The alignment was compensated so that the accelerometers were aligned as they would be in a THOR-Lx foot, with the x-axis parallel to the ground. A bi-axial accelerometer was mounted at the intersection of the distal third and proximal two thirds of the tibia (the same position as in the THOR-Lx). This was also adjusted so that the alignment was the same as for the dummy leg. A single uni-axial accelerometer was mounted on the upper tibia, in the z plane on the sulcus behind the patella tendon attachment. A single uni-axial accelerometer was mounted on the dummy femur

on top of a standard Hybrid III 6-axis load cell, aligned to the x-axis of the femur.

In addition to this instrumentation, a 5-axis load cell was implanted into the tibia for each of the first two pilot specimens. This was undertaken using the method documented by Manning et al. [1997a]. This was used to determine the relationship between the force measured under the foot and the force at the mid-tibia, so that the severity range for the main test programme could be determined. This load cell was not used for the main test programme to avoid disruption of the tibia to maintain a biofidelic limb mass and stiffness.

Test Protocol

The sled deceleration honeycomb used was 0.276 MPa with a 19 mm cell size, and was 320 mm wide, 150 mm tall and 600 mm deep. The foot-plate honeycomb was 1.793 MPa with a cell size 6.35 mm, and was 100 mm tall and 200 mm deep. The width of the foot-plate honeycomb was varied between 40 and 200 mm to give the range of foot impact forces required. Eight elastic cords were used with a pull-back distance of 5.0 m to give an impact velocity of approximately 12 ms^{-1}.

The potted specimen was attached to the femur load cell and the lateral position of the hip joint adjusted such that the tibia was in line with the direction of travel and the natural angle of the femur was preserved. Free flexion and extension at the hip was maintained.

The slack in the knee brace was then taken up to pre-load the specimen and the Achilles tendon was tensioned to 500 N. This gave a combined load under the foot of approximately 870 N, almost all of which was applied through the pedal representation. This is comparable to the pedal forces recorded in emergency braking simulations in previous work [Manning et al., 1997b; Palmertz et al., 1998]. The stability of the foot on the pedal was then checked. If necessary, the Achilles tension was removed, the position of the foot on the pedal adjusted and the loading sequence repeated. Once the position of the foot was stable under load, the sled was winched back and the test fired.

Statistical Design

Tests were performed at five impact severities. These were chosen such that the highest and lowest severities were likely to be predominantly injury and non-injury producing, with the middle groups providing a mixture of injury and non-injury data. The number of specimens in each group was unequal as the later tests were allocated to the moderate severities that the earlier tests had indicated would have a more uncertain outcome. This adaptive approach has a greater statistical power than testing at two severities (expected injury and non-injury), although there is a greater chance of it not providing a statistically significant result. The specimens for each group were randomised prior to any testing or bone mineral density (BMD) analysis.

THOR-Lx Tests

The THOR-Lx was tested at the same severities of impact with the same test configuration as the PMHS specimens. The knee brace and external Achilles tension were not used as these represented active muscle tone that a human would have in a crash, but which would not be simulated in a crash test dummy in a full-scale car crash test. The position of the THOR-Lx foot on the pedal and the joint angles at the ankle and knee were the same as for the PMHS tests. The tension of the Achilles spring cable was adjusted as described in the THOR user manual.

RESULTS

Table 1 (Appendix 1) shows the physical data for the PMHS specimens used in this programme. The mean age of the specimens was 75.8 years (σ 5.2 years - the age of one specimen was not known). The mean tibia BMD was 0.653 $g.cm^{-2}$ (σ 0.293 $g.cm^{-2}$) and the mean large calcaneal BMD was 0.500 $g.cm^{-2}$ (σ 0.199 $g.cm^{-2}$). The results of the PMHS tests are shown in Table 2 (Appendix 1). This shows the peak footplate accelerations and the resulting forces measured under the foot in the direction of the Z-axis of the tibia, along with a description of the injuries generated.

The severity of impact (hereafter described in terms of the width of foot-plate honeycomb used to load the foot) is shown in Figure 7. The highest severity (200 mm of foot-plate honeycomb) corresponds well with the target pulse.

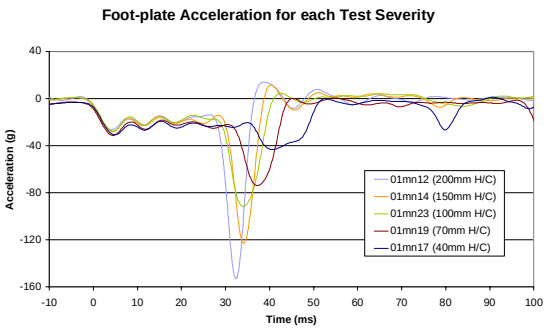

Figure 7. Variation of foot-plate deceleration (test severity) for different widths of foot-plate honeycomb.

Figure 8 shows the mean mid-foot and heel forces, together with the range for each, for moderate severity tests with 100 mm of foot-plate honeycomb. It shows that the force applied to the heel was very low compared to the force applied to the mid-foot. The ratio of heel to mid-foot force varied with the test severity, but a minimum of two-thirds of the force was applied to the mid-foot in all the tests. The graph also shows the repeatability of the PMHS tests. The initial load at the mid-foot (between -10 and 0 ms) is due to the pre-loading (Achilles tension and knee brace), simulating the muscular forces in pre-impact braking.

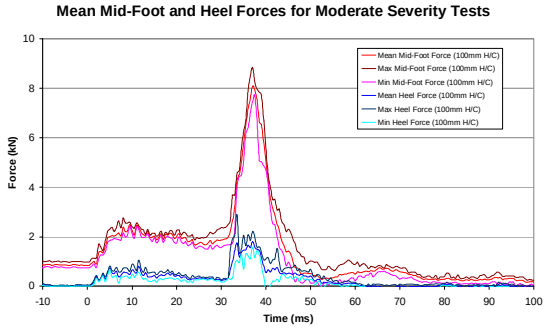

Figure 8. Comparison of mid-foot and heel forces at tests with 100 mm honeycomb (moderate severity).

Most of the injuries generated were calcaneus fractures, although other hard tissue injuries (talar neck fracture, damage to the anterior margin of the distal tibial cortex, fracture of the posterior spur of the talus and damage to the lateral margin of the articular surface of the talus) and a soft tissue injury (rupture of the anterior talo-fibular ligament) were recorded. Some injuries to the proximal tibia, knee joint and a fracture of the second metatarsal at the accelerometer mounting point were also identified, but were not considered as injuries for the definition of the ankle and foot injury risk curve. Figure 9 shows the injuries to specimen 2-05L, which included a talar neck fracture and an intra-articular fracture of the calcaneus. Damage to the distal tibial cortex in this specimen was not visible on the x-ray, but became apparent during the necropsy.

Table 3 (Appendix 1) shows the results of the THOR-Lx tests at the same severities as the PMHS tests. It shows mean peak forces, moments and accelerations at each test severity. The repeatability of the THOR-Lx responses are shown in Figure 10, which shows the lower tibia Fz for three tests at the same severity.

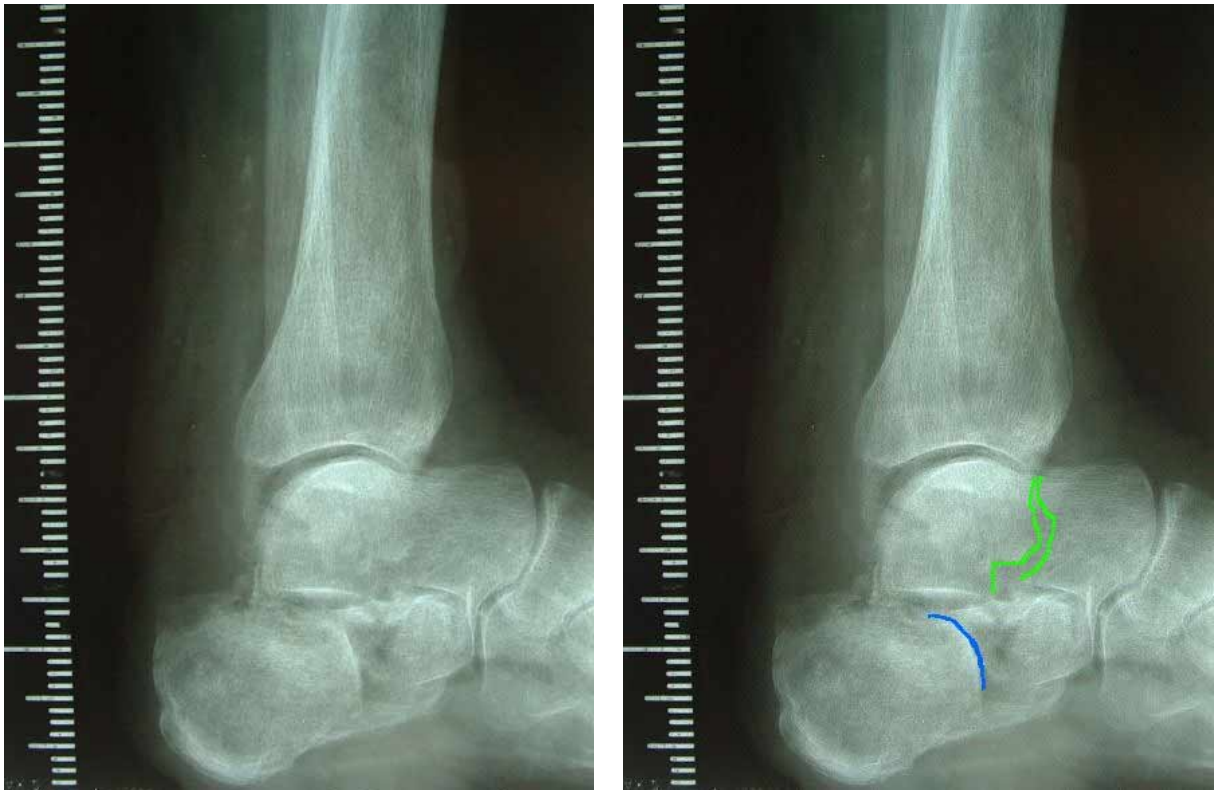

Figure 9. Specimen 2-05L - talar neck fracture (green) and intra-articular fracture of the calcaneus (blue).

Two tests were undertaken with the THOR-Lx with the force-limited knee restraint as used in the PMHS tests and two with a flat foot-plate (no pedal representation) in order to gauge the effect that these changes had on the THOR-Lx measurements. The knee restraint was found to increase moderately the lower tibia Fz, with the effect being greater at higher foot loading severity (Figure 11). The use of the pedal representation had little effect on the lower tibia Fz (Figure 12).

A probit analysis of average THOR-Lx measurements at each test severity compared with ankle and foot injuries in PMHS tests at the same severity was performed. Additional factors such as BMD were also included in the analysis, but these did not yield statistically significant results. Only upper and lower tibial axial force (Fz) yielded statistically significant relationships with injury. There was no correlation between specimen physical characteristics (such as age and mass) and injury or test severity.

The probability of ankle or foot injury versus THOR-Lx lower tibial axial load (Fz) is shown in Figure 13, along with the 95th percentile confidence limits. The proximity of the lower tibial load cell to the ankle makes it a logical choice for an injury criteria for the foot and ankle, even though both upper and lower THOR-Lx tibial Fz are significantly correlated with injury and have similar confidence limits.

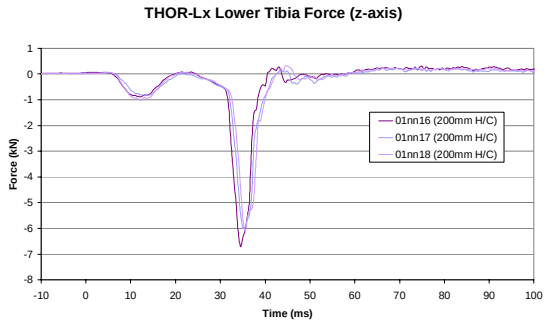

Figure 10. Repeatability of the THOR-Lx lower tibia Fz response in tests with 40 mm honeycomb.

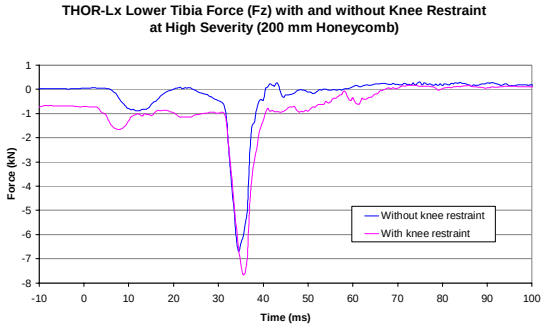

Figure 11. THOR-Lx lower tibia Fz with and without knee restraint.

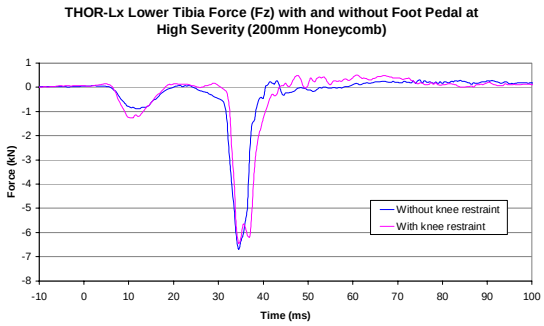

Figure 12. THOR-Lx lower tibia Fz with and without pedal representation.

DISCUSSION

One of the aims of this study was to produce a series of foot and ankle injuries through axial loading that would be representative of those injuries observed in road traffic accidents that lead to long term impairment. These were primarily fractures to the os calcis, talus and distal tibia (pilon). This was achieved with a dual-impact sled system that reproduced both the vehicle deceleration phase and the footwell intrusion phase of a frontal impact. The deceleration pulse and the load applied to the foot were highly repeatable with dummy legs and with PMHS specimens.

In preliminary testing, it was demonstrated that impacts with a flat foot-plate generated injuries not consistent with those found in accident studies or seen in clinical practice. High-speed film analysis of these tests indicated that the foot had flattened out when loaded, causing tension in the plantar fascia and the long plantar ligaments. It is thought that during the impact the tension became sufficiently high that the attachment of the long plantar ligament to the antero-inferior cortex of the calcaneus was fractured. This fracture dramatically weakened the calcaneus and allowed the impact to cause further damage to the calcaneus.

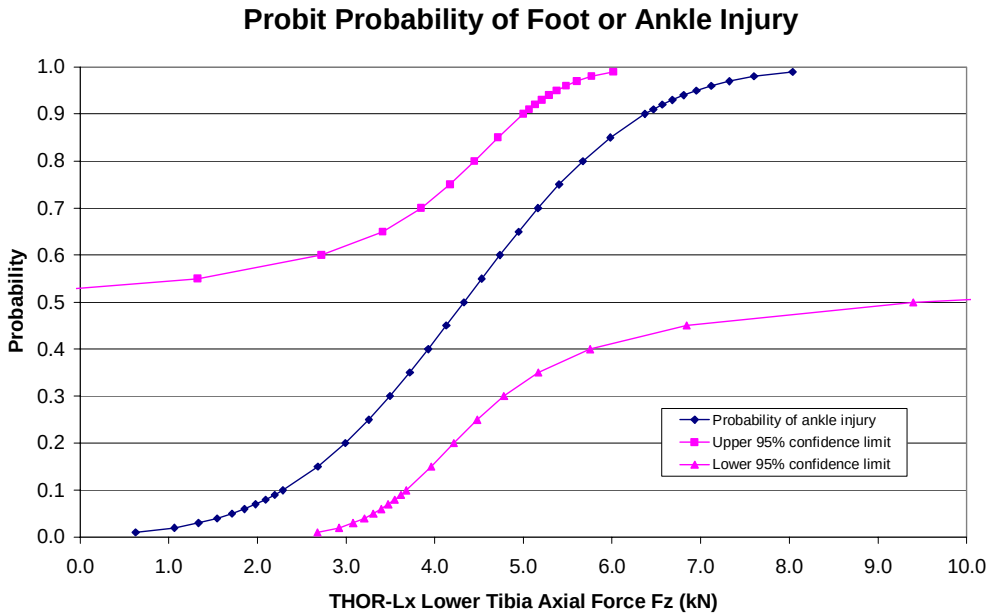

Figure 13. Probability of foot or ankle injury for the THOR-Lx lower tibia Fz.

As a result, the test rig was modified to apply loads predominantly to the mid-foot, via a representation of a brake pedal. Full-scale vehicle tests have shown that the feet of the dummy move forwards and upwards during the initial vehicle deceleration phase such that the mid-foot is on the brake pedal at impact. This is also similar to the foot position found in studies that have been most successful in generating talus and pilon fractures [Kitagawa et al., 1998; McMaster et al., 2000]. However, both of these used rigidly potted below-knee specimens, which is not representative of the in-car situation. In this test programme, using a sled system to reproduce the vehicle deceleration and footwell intrusion pulses to an above-knee specimen with freedom to articulate normally, fractures of the calcaneus predominate. Whilst clinical studies report that fractures to the calcaneus commonly occur, pilon fractures and Lis-franc fracture dislocations are a significant proportion of foot and ankle injuries [Morris et al., 1997; Funk et al., 2001].

All the specimens used were assessed for bone mineral density by dual-energy X-ray absorbtiometry (DEXA). Density is a good predictor of the stiffness of cancellous bone and subsequently strength, provided the bone is reasonably uniform [Hodgskinson and Currey, 1993]. Thus, lower failure thresholds for specimens with low densities can be expected. The average BMD for the cohort in the present study, with an average specimen age of 76 years, was lower than that found in the previous PMHS work by our group, which had an average specimen age of 68 years. It is not known how the BMD values compare with the population as BMD measurements at the sites used are not commonly taken. However, an injury criterion based on PMHS tests with an elderly cohort should give a conservative estimate of the risk of injury to the population in general.

Two of the specimens fractured at a low threshold of input loading and they recorded two of the three lowest mineral densities of the sample. It is difficult to know how significant these two results are in such a small series of tests. It is suspected that their failure was largely a result of the low mineral density in each. Interestingly although they failed at a low threshold, the fractures created were of less clinical significance than those created at higher peak forces.

The dominance of calcaneus fractures may be because the bone mineral density of the distal tibia was higher than that of the calcaneus for this sample (0.653 $g.cm^{-2}$ compared with 0.500 $g.cm^{-2}$). It is also possible that without recreating the dynamic support for the arch of the foot, through the action of all of the muscles that have this function, the role of the fore-foot under load and its transmission of that load to the distal tibia is being undervalued. Previous tests have also indicated that pilon fractures become more common as impact forces and Achilles tension increase [McMaster et al., 2000]. The relatively low impact and Achilles forces used in some of the current tests may have

been insufficient to stimulate pilon fractures. However, a number of injuries to the talus (including talar neck and articular surface fractures) and many severe fractures of the articular surface of the calcaneus were produced. These are associated with poor outcome and long-term impairment [Taylor et al., 1997] and are appropriate targets for prevention using an injury risk criterion. It is suggested that an injury criterion based predominantly on calcaneus injury should be conservative and offer protection from e.g. talus and pilon fractures.

Injuries to the calcaneus have been attributed to heel-slap, whereby the heel is not initially in contact with the footwell but is loaded suddenly and severely by the intruding footwell during the impact. Figure 8 shows the mid-foot (pedal) and heel forces measured in the moderate severity tests with 100 mm of aluminium honeycomb to load the foot. A similar pattern was seen in all tests, with a minimum of two thirds of the total force being applied to the mid-foot in all tests. No evidence for heel-slap was found.

Previous work has suggested high forces for injury. Kitigawa et al. [1998] reported an average failure load, measured at the distal tibia, was 8.1 kN for calcaneus fracture and 7.3 kN for pilon fracture. These tests used a high rate of loading and a rigidly mounted below-knee specimen that was unable to move away from the impact. A 50% risk of injury at an impactor force of 6.8 kN was reported by Yoganandan et al. [1996]. Again, these used a rigidly potted below knee specimen, impacted by a pendulum, but the specimen was attached to a sled that was able to react to the impact. Funk et al. [2001] reported the axial loads at an implanted tibial load cell. The above-knee specimens were mounted horizontally in a rig with the knee at 90° and constrained in an adjustable, padded block. This allowed some movement of the specimen, whilst allowing sufficiently high forces for injury generation. The risk of injury for 45 or 65 year-old males and females was given as a function of the measured tibial load. The axial force associated with a 50% risk of injury was as much as 2 kN higher for a 45 year-old compared to a 65 year-old, but was less than 4 kN for a 65 year-old female and approximately 8 kN for a 45 year old male, assuming no Achilles tension.

None of these results are directly comparable with the THOR-Lx injury risk curve presented in this paper as they all give the risk of injury in the human. However, in our test series the mean peak foot-plate force for those tests where a serious injury was induced was 8.6 kN. The data obtained in this study indicates a 50% risk of serious ankle or foot injury at a THOR-Lx lower tibial axial force (Fz) of 4.3 kN. It should be noted that all of the PMHS specimens in this study were instrumented such as to preserve the biofidelity of the specimens.

CONCLUSIONS

A sled rig has been developed that is able to load the lower limb in a manner representative of the loading in frontal impact car crashes.

The rig has been used to impact fourteen fresh-frozen PMHS specimens at a range of severities to investigate the tolerance of the foot and ankle to axial loading.

A range of injuries has been generated, including many that have been identified as a priority for prevention such as calcaneus, talar neck and pilon fractures.

The injuries have been predominantly intra-articular fractures, which are difficult to treat clinically and which are likely to lead to long-term impairment.

The tests have been repeated using a THOR-Lx advanced lower extremity, which can be retro-fitted to the existing regulatory frontal impact dummy, the Hybrid-III.

An injury risk curve for the THOR-Lx, giving the risk of severe foot or ankle injury for a given lower tibia axial force (Fz) has been proposed.

A lower tibial axial force (Fz) in the THOR-Lx is associated with a 50% risk of serious foot or ankle injury.

ACKNOWLEDGEMENTS

The work described in this report forms part of a major biomechanics project funded by the UK Department for Transport and the EC ‘Competitive and Sustainable Growth’ project ‘Improved Frontal Impact Protection through a World Frontal Impact Dummy (FID)’. The authors also wish to express their gratitude for the valuable contributions of Mr B Sexton of TRL Limited and Professor R Roberts of McMaster University in the statistical design of the experiment, Mr Les Wall of TRL Limited in the design and fabrication of the sled rig and Mr M Parry of the University of Nottingham in the PMHS testing.

REFERENCES

Burgess A, Dischinger P, O'Quinn T and Schmidhauser C (1995). “Lower extremity injuries in drivers of airbag equipped automobiles: clinical

and crash reconstruction correlations." *J Trauma* **38**: 509-516.

Crandall J (1994). The preservation of human surrogates for biomechanical studies. Faculty of Engineering and Applied Science. Charlottesville, University of Virginia**:** 271.

Crandall J, Portier L, Petit P, Hall G, Bass C, Klopp G, Hurwitz S, Pilkey W, Trosseille X, Tarrière C and Lassau J-P (1996). Biomechanical response and physical properties of the leg, foot, and ankle. *40th Stapp Car Crash Conference*, Albuquerque, New Mexico, USA: Society of Automotive Engineers, Warrendale, PA, USA, 962424, 173-192.

Funk J, Crandall J, Tourret L, MacMahon C, Bass C, Khaewpong N and Eppinger R (2001). The effect of active muscle tension on the axial injury tolerance of the human foot/ankle complex. *17th International Technical Conference on the Enhanced Safety of Vehicles*, Amsterdam, The Netherlands: US Dept of Transport, National Highway Traffic Safety Administration, 237,

Hodgskinson R and Currey J (1993). "The separate effects of osteoporosis and density on the strength and stiffness of human cancellous bone." *Clinical Biomechanics* **8**: 262-268.

Kitagawa Y, Ichikawa H, King A and Levine R (1998). A severe ankle and foot injury in frontal crashes and its mechanism. *42nd Stapp Car Crash Conference*, Tempe, Arizona, USA: Society of Automotive Engineers, Warrendale, PA, USA, 983145, 1-12.

Kruger H, Heuser G, Kraemer B and Schmitz A (1994). Foot loads and footwell intrusion in an offset frontal crash. *14th International Technical Conference on the Enhanced Safety of Vehicles*, Munich, Germany: US Dept of Transport, National Highway Traffic Safety Administration, 94-S4-0-03, 528-534.

Manning P, Roberts A, Owen C, Lowne R and Wallace W (1997a). Long bone load cell instrumentation: a revised technique. *25th International Workshop on Human Subjects for Biomechanical Research*, Lake Buena Vista, Florida, USA: National Highway Traffic Safety Administration, 1-14.

Manning P, Roberts A, Owen C, Lowne R and Wallace W (1997b). The position and movement of the foot in emergency manoeuvres and the influence of tension in the Achilles tendon. *41st Annual Stapp Car Crash Conference*, Lake Buena Vista, Florida, USA: Society of Automotive Engineers, Warrendale, PA, USA, 973329, 195-206.

Martin P, Crandall J, Pilkey W and Miller T (1997). Passenger car drivers: annual injury incidence and costs projected to 2005. *41st Association for the Advancement of Automotive Medicine*, Orlando, Florida, USA: AAAM, 249-265.

McMaster J, Parry M, Wallace W, Wheeler L, Owen C, Richard Lowne R, Oakley C and Roberts A (2000). Biomechanics of ankle and hindfoot injuries in dynamic axial loading. *44th Stapp Car Crash Conference*, Atlanta, Georgia, USA: Society of Automotive Engineers, Warrendale, PA, USA, 2000-01-SC23, 357-377.

Morris A, Thomas P, Taylor A and Wallace W (1997). Mechanisms of fracture in ankle and hind-foot injuries to front seat car occupants: an in-depth accident data analysis. *41st Stapp Car Crash Conference*, Lake Buena Vista, Florida, USA: Society of Automotive Engineers, Warrendale, PA, USA, 973328, 181-194.

Otte D (1996). Biomechanics of lower limb injuries of belted car drivers and the influence of intrusion and accident severity. *40th Stapp Car Crash Conference*, Albuquerque, New Mexico, USA: Society of Automotive Engineers, Warrendale, PA, USA, 962425, 193-206.

Owen C and Hynd D (2001). FID accident analysis part 1. TRL Limited

Palmertz C, Jakobsson L and Karlsson A-S (1998). Pedal use and foot positioning during emergency braking. *IRCOBI*, Goteborg: IRCOBI, 135-146.

Pattimore D, Ward E, Thomas P and Bradford M (1991). The nature and cause of lower limb injuries in car crashes. *35th Stapp Car Crash Conference*, San Diego, California, USA: Society of Automotive Engineers, Warrendale, PA, USA, 912901, 177-188.

Pilkey W, Sieveka E, Crandall J and Klopp G (1994). The influence of foot placement and vehicular intrusion on occupant lower limb injury in full-frontal and frontal-offset crashes. *14th International Technical Conference on the Enhanced Safety of Vehicles*, Munich, Germany: US Department of Transportation, National Highway Traffic Safety Administration, 94-S4-W-31, 734-741.

Sakurai M (1996). An analysis of injury mechanisms for ankle/foot region in offset frontal collisions. *40th Stapp Car Crash Conference*, Albuquerque, New Mexico, USA: Society of Automotive Engineers, Inc., Warrendale, Pennsylvania, USA, 962429,

Sherwood C, O'Neill B and Hurwitz S (1999). Lower extremity injury causation in frontal crashes. *IRCOBI Conference*, Sitges, Spain: IRCOBI, 513-524.

Taylor A, Morris A, Thomas P and Wallace A (1997). Mechanisms of lower extremity injuries to front seat car occupants: an in-depth accident

analysis. *IRCOBI*, Hannover, Germany: IRCOBI, 53-72.

Yoganandan N, Pintar F, Boynton M, Begeman P, Prasad P, Kuppa S, Morgan R and Eppinger R (1996). Dynamic axial tolerance of the human foot-ankle complex. *40th Stapp Car Crash Conference*, Albuquerque, New Mexico, USA: Society of Automotive Engineers, Inc., Warrendale, Pennsylvania, USA, 962426, 207-218.

APPENDIX A

Table 1.
PMHS physical data

Specimen ID	Sex	Age (years)	Mass (g)	Knee centre to ankle center (mm)	Foot length (mm)	Heel flesh depth (mm)	Tibia BMD ($g.cm^{-2}$)	L Cal BMD ($g.cm^{-2}$)	S Cal BMD ($g.cm^{-2}$)
2-05L	F	82	2190	375	217	13	0.549	0.266	0.258
2-04L	M	77	3427	418	284	18	0.602	0.468	0.449
2-07L	M	68	3860	410	243	18	0.958	0.579	0.545
2-04R	M	77	3640	415	272	18	0.726	0.484	0.451
2-01R	F	*	2362	328	225	11	0.687	0.479	0.44
2-14L	M	79	4183	405	263	15	0.999	0.88	0.833
2-12R	M	71	3256	415	253	18	0.329	0.515	0.508
2-05R	F	82	2146	364	223	16	0.359	0.312	0.306
2-10L	M	78	2440	367	229	14	0.212	0.225	0.209
2-10R	M	78	2521	370	240	14	0.261	0.251	0.241
2-14R	M	79	4421	403	265	16	1.127	0.817	0.762
2-11R	M	67	4428	405	262	18	0.994	0.670	0.667
2-01L	F	*	2323	325	229	13	0.667	0.481	0.476
2-12L	M	71	3314	418	248	15	0.669	0.566	0.536
Average		*75.8*	*3179*	*387*	*247*	*16*	*0.653*	*0.500*	*0.447*
Std Dev		*5.2*	*846*	*32*	*21*	*2*	*0.293*	*0.199*	*0.188*

* Age not known.

Table 2.
PMHS test results

Specimen ID	Honeycomb Width (mm)[†]	Peak Axial Foot Force (kN)[‡]	Peak Foot-plate Acceleration (g)	Injury
2-05L	200	10.43	147.2	Comminuted intra-articular fracture calcaneus + fracture neck and body of talus + damage to anterior margin of distal tibial cortex and articular margin + incomplete fracture medial malleolus + comminuted fracture of lateral malleolus
2-04L	200	11.20	152.7	Intra-articular fracture calcaneus including sinus tarsi
2-07L	200	11.72	147.7	Comminuted intra-articular fracture calcaneus + fracture of posterior spur of talus
2-04R	150	9.87	122.6	Intra-articular fracture calcaneus + rupture of anterior talo-fibular ligament
2-01R	40	4.25	43.1	No injury
2-14L	40	4.58	38.9	No injury
2-12R	70	6.23	73.6	No injury
2-05R	70	5.10	83.5	Comminuted intra-articular fracture calcaneus + lateral margin of inferior articular surface of talus damaged
2-10L	70	5.24	90.9	Comminuted intra-articular fracture calcaneus
2-10R	40	3.95	48.8	No injury
2-14R	100	9.59	91.6	No injury
2-11R	100	9.71	112.1	No injury
2-01L	70	6.65	70.3	Fracture posterior spur of the talus + intra-articular fracture calcaneus + fracture of the proximal pole of the cuboid
2-12L	70	6.63	68.5	No injury

[†] Analogous to foot impact severity
[‡] Along the axis of the tibia

Table 3.
THOR-Lx test results

	Impact Severity				
	Low				High
Honeycomb width (mm)	40	70	100	150	200
Number of tests	4	3	3	3	3
Av. Lower Tibia Fz (kN)	1.93	3.82	5.09	6.43	6.25
Av. Lower Tibia Fx (kN)	0.28	0.46	0.72	0.71	0.64
Av. Lower Tibia My (Nm)	36.9	65.8	100.0	107.5	101.8
Av. Upper Tibia Fz (kN)	1.23	2.58	3.61	4.59	5.37
Av. Upper Tibia My (Nm)	29.4	50.2	77.7	86.4	94.9
Av. Lower Tibia Ax (g)	34.8	62.1	98.1	119.7	120.0
Av. Upper Tibia Az (g)	45.6	75.0	107.4	120.4	137.8
Av. Foot Az (g)	48.7	82.7	116.7	152.9	229.4
Av. Foot Ax (g)	62.9	104.8	162.9	262.3	358.8